

Scaling of the Irreducible SO(3)-Invariants of Velocity Correlations in Turbulence

Siegfried Grossmann,¹ Detlef Lohse,^{1,2} and Achim Reeh¹

Received February 8, 1998; final May 8, 1998

The scaling behavior of the SO(3) irreducible amplitudes $d_n^l(r)$ of velocity structure tensors is numerically examined for Navier–Stokes turbulence. Here, l characterizes the irreducible representation by the index of the corresponding Legendre polynomial, and n denotes the tensorial rank, i.e., the order of the moment. For moments of different order n but with the same representation index l extended self-similarity (ESS) towards large scales is found. Intermittency seems to increase with l . We estimate that a crossover behavior between different inertial subrange scaling regimes in the longitudinal and transversal structure functions will hardly be detectable for achievable Reynolds numbers.

KEY WORDS: Fully developed turbulence; SO(3) invariants of velocity correlations; scaling exponents; intermittency; longitudinal vs. transversal velocity structure functions.

The most fundamental objects to analyze the structure of turbulent velocity fields $\mathbf{u}(\mathbf{x}, t)$ are the tensorial moments of the velocity differences $v_i(\mathbf{r}; \mathbf{x}, t) = u_i(\mathbf{x} + \mathbf{r}, t) - u_i(\mathbf{x}, t)$, averaged over time t or/and position \mathbf{x} , considered as functions of scale \mathbf{r} ,

$$D_{i_1, i_2, \dots, i_n}(\mathbf{r}) = \langle v_{i_1} v_{i_2} \cdots v_{i_n} \rangle \quad (1)$$

If the eddy size $r = |\mathbf{r}|$ is in the inertial subrange (ISR), i.e., $\eta \ll r \ll L$, algebraic scaling of the moments is expected. Here, η is the inner (Kolmogorov) scale and L the external length scale.⁽¹⁾ If the turbulent flow

¹ Fachbereich Physik der Universität Marburg, D-35032 Marburg, Germany; e-mail: grossmann_s@physik.uni-marburg.de, reeh@mail.uni-marburg.de.

² Present address: University of Twente, Department of Applied Physics, P.O. Box 217, 7500 AE Enschede, The Netherlands; e-mail: lohse@tn.utwente.nl.

field can be considered as statistically isotropic (or close to), one better uses rotational invariants instead of the tensorial components, in order to cope with the multitude of scaling exponents. The most commonly used invariants are the structure functions of the longitudinal velocity component $v_L = \mathbf{v} \cdot \mathbf{r}^0$ and the transversal velocity $\mathbf{v}_T = \mathbf{v} - v_L \mathbf{r}^0$; here, \mathbf{r}^0 denotes the unit vector in \mathbf{r} direction. We denote these structure functions as

$$D_n^L(r) = \langle [v_L(\mathbf{r}; \mathbf{x}, t)]^n \rangle \propto r^{\zeta_n^L} \quad (2)$$

$$D_n^T(r) = \langle |\mathbf{v}_T(\mathbf{r}; \mathbf{x}, t)|^n \rangle \propto r^{\zeta_n^T} \quad (3)$$

each is assumed to scale in the ISR with the corresponding exponents ζ_n^L and ζ_n^T . A third convenient structure function is the n th order moment of the *modulus* of the eddy velocity difference $\mathbf{v}(\mathbf{r}; \mathbf{x}, t)$ which again is assumed to scale as

$$D_n^M(r) = \langle |\mathbf{v}(\mathbf{r}; \mathbf{x}, t)|^n \rangle \propto r^{\zeta_n^M} \quad (4)$$

Traditionally, it was believed that all three scaling exponents are the same, $\zeta_n = \zeta_n^M = \zeta_n^L = \zeta_n^T$. But recent advances in experimental technology⁽²⁻⁵⁾ and computational power and technique^(6,7) raised increasing doubts if this is true for general moments of order n , as it is for the most often considered 2nd order structure function, $n=2$, where the condition of incompressibility enforces $D_2^L \propto D_2^T \propto D_2^M \propto r^{\zeta_2}$. For general n , it was found in several experiments and simulations that the degree of intermittency (i.e., the deviations of the scaling exponents from the classical value $\zeta_n = n/3$) is considerably larger in the transversal moments compared to the longitudinal ones; for a summary of the results see Table 1 of ref. 7.

In a recent paper, L'vov, Podivilov, and Procaccia⁽⁸⁾ suggested that it was not the longitudinal or the transversal structure functions that obey clean algebraic scaling, but rather the amplitudes of the moment tensor Eq. (1) decomposed into the irreducible representations of the rotation group SO(3),

$$d_n^l(r) \propto \langle (v^2(\mathbf{r}; \mathbf{x}, t))^{n/2} P_l(\mathbf{v}^0 \cdot \mathbf{r}^0) \rangle \propto r^{\zeta_n^l} \quad (5)$$

The representation label l runs through $0 \leq l \leq n$ with the same parity as n , if statistical reflection symmetry of the turbulent flow field is guaranteed⁽⁸⁾; P_l is the Legendre polynomial. The amplitude of the unity representation, $d_n^0(r)$, is already part of the conventional set of structure functions, since $d_n^0(r) \propto D_n^M(r)$.

For the second and fourth order structure tensors, the amplitudes $d_2^l(r)$ and $d_4^l(r)$ are linear combinations of the longitudinal, transversal,

and modulus structure functions. We follow L'vov *et al.*'s definitions⁽⁸⁾ $a_0 = d_2^0$, $a_2 = d_2^2$, $c_0 = d_4^0$, $c_2 = d_4^2$, $c_4 = d_4^4$ obtaining

$$\begin{pmatrix} a_0 \\ a_2 \end{pmatrix} = \begin{pmatrix} \frac{1}{3} & 0 \\ \frac{1}{6} & -\frac{1}{2} \end{pmatrix} \begin{pmatrix} D_2^M \\ D_2^L \end{pmatrix} \quad (6)$$

$$\begin{pmatrix} c_0 \\ c_2 \\ c_4 \end{pmatrix} = \begin{pmatrix} \frac{1}{\sqrt{5}} & 0 & 0 \\ \frac{1}{2\sqrt{7}} & \frac{3}{2\sqrt{7}} & -\frac{3}{2\sqrt{7}} \\ \frac{-6}{\sqrt{70}} & \frac{10}{\sqrt{70}} & \frac{15}{\sqrt{280}} \end{pmatrix} \begin{pmatrix} D_4^M \\ D_4^L \\ D_4^T \end{pmatrix} \quad (7)$$

On the rhs also other ways of representing the n-rank velocity correlation tensor can alternatively be given, using e.g. D_2^T in (6) or mixed transversal/longitudinal moments in (7) as done in Eq. (13.81) of ref. 1 or in ref. 9 which uses $D_{11} = D_2^L$, $D_{22} = D_2^T/2$, $D_{1111} = \langle v_1^4 \rangle = D_4^L$, $D_{1122} = \langle v_1^2 v_2^2 \rangle$, and $D_{2222} = \langle v_2^4 \rangle = 3D_{2233} = 3D_4^T/8$, where the 1-axis has been put in the longitudinal direction parallel to \mathbf{r} . For these structure functions we obtain

$$\begin{pmatrix} c_0 \\ c_2 \\ c_4 \end{pmatrix} = \begin{pmatrix} \frac{1}{\sqrt{5}} & \frac{4}{\sqrt{5}} & \frac{8}{3\sqrt{5}} \\ \frac{2}{\sqrt{7}} & \frac{2}{\sqrt{7}} & -\frac{8}{3\sqrt{7}} \\ \sqrt{\frac{8}{35}} & -12\sqrt{\frac{2}{35}} & \sqrt{\frac{8}{35}} \end{pmatrix} \begin{pmatrix} D_{1111} \\ D_{1122} \\ D_{2222} \end{pmatrix} \quad (8)$$

The point of L'vov *et al.* is that the invariants a_l, c_l on the lhs of Eqs. (6), (7), and (8) are *distinguished* because the $d_n^l(\mathbf{r})$ are the amplitudes of the structure tensor for its decomposition into the components of the *irreducible representations* of the rotational symmetry group SO(3).

In this paper we present the scaling properties of the *fourth* order moments $d_4^l(\mathbf{r})$ from a full numerical simulation of the Navier–Stokes equation on a 96^3 grid with periodic boundary conditions. The numerical turbulence is forced on the largest scales, the averaging time is about 120 large eddy turnovers, and the Taylor–Reynolds number is $Re_\lambda = 110$. We also performed a simulation with $Re_\lambda = 75$ which lead to the same results. The isotropy of the flows has carefully been checked; for details of the simulations we refer to ref. 7.

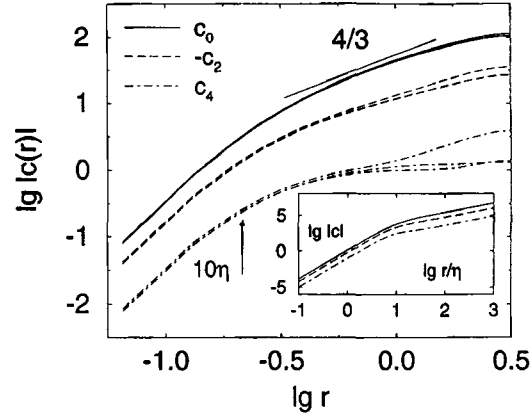


Fig. 1. Fourth order structure functions $c_{0,2,4}(r)$ as functions of r . The inset shows $c_{0,2,4}(r)$ (top to bottom) as they follow from the Batchelor parametrization (9) and Eqs. (2) of ref. 9. The different magnitudes and the distinct transitional behavior of the different irreducible representations can be recognized. Note that the local slope of $\log_{10} c_4(r)$ vs $\log_{10} r$ around the transition is *not* monotonous. By assumption the ISR scaling exponents are the same.

The *second* order moments all asymptotically scale the same because of incompressibility. Assuming classical scaling $\zeta_2 = 2/3$ one obtains $D_2^L = 4D_2^T/3$ and $a_0 = 11a_2 = D_2^M/3$. In Fig. 1 we give the *fourth* order structure functions $c_{0,2,4}(r)$. As tested for smaller Reynolds numbers and longer averaging times, the wiggle in $c_4(r)$ at large r is not statistically safe. It seems that very long averaging times are necessary for moments with large l to converge at large scales.³ As expected for this low Re_λ , the scaling properties of these structure functions $c_{0,2,4}(r)$ is very poor, because there is not yet a well developed ISR. There is analytical behavior $\propto r^4$ in the viscous subrange (VSR) followed by a transition and leveling off in the inertial and stirring subrange around $r \sim L$. What can be said, however, is that with increasing l (i) the magnitude of $c_l(r)$ decreases and (ii) the degree of intermittency seems to increase, $\zeta_4^4 < \zeta_4^2 < \zeta_4^0 < 4/3$. The reason for (i) is that c_0 is a *sum* of positive definite structure functions, whereas c_2 and the more c_4 are *differences* thereof, similar to $a_2 = (D_{22} - D_{11})/3$ which also is much smaller than $a_0 = D_{11} + 2D_{22}$. The reason for (ii) presumably is that larger l in (5) means the probing of smaller scale structures which are traditionally associated with stronger intermittency.

Fortunately, the extended self similarity method (ESS,⁽¹⁰⁾) allows for more quantitative statements. Here, we focus on the scaling of the fourth order structure functions vs second order ones. More specifically, to visualize

³ Chen *et al.*⁽⁶⁾ noted that transverse structure functions are more difficult to converge.

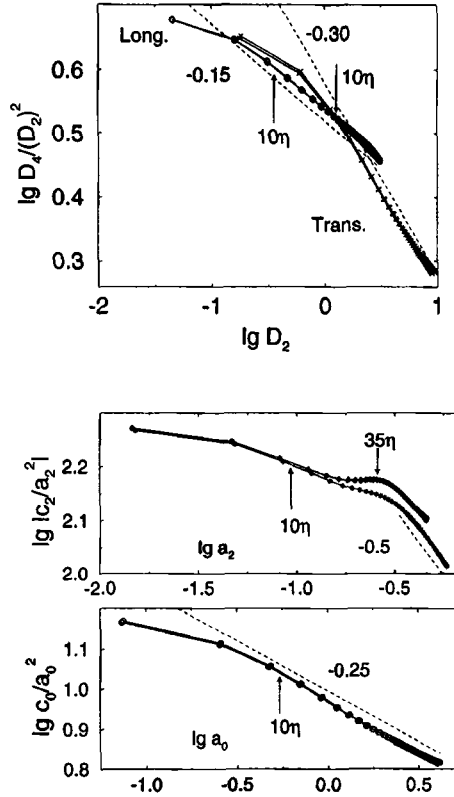


Fig. 2. Compensated ESS plots for different space directions of fourth vs second order structure functions, giving the ISR scaling exponent $\rho_i = (\zeta_4^i - 2\zeta_2^i)/\zeta_2^i$. The plot c_2/a_2^2 vs a_2 displays a distinct bump around 35η for all three space directions, though it is slightly differently developed in strength, possibly because of the unavoidable anisotropy in the forcing, possibly because of the too short averaging time (Fig. 2b, upper). Convergence is much less a problem in the ESS plot c_0/a_0^2 vs a_0 (Fig. 2b, lower) and consequently also in the ESS plots of the longitudinal and transversal structure functions where the rank zero contributions dominate (Fig. 2a).

the deviations from classical scaling we calculate *compensated* ESS plots $D_4^i/(D_2^i)^2$ vs D_2^i , $i = L, T, M$, and $d_4^l/(d_2^l)^2$ vs d_2^l , $l = 0, 2$, see Fig. 2. For $l = 0$ we find ESS scaling from $r \sim 10\eta$ up to $r \sim L$, resembling the ESS scaling for the longitudinal and transversal structure functions Fig. 2a which was extensively analyzed in refs. 10 and 11. For $l = 2$ we find ESS towards large scales $r \gtrsim 50\eta$, but *no ESS towards smaller scales* $r < 50\eta$. Instead, there is a bump in the curve c_2/a_2^2 vs a_2 for $r \sim 35\eta$. As this feature is very unusual, we checked very carefully whether the bump would smooth

for increasing averaging time. This is *not* the case. It also persists for a different type of large scale forcing and smaller Reynolds number, but much larger averaging time.

At first sight, the bump was a surprise to us. However, we suggest that it can be understood as a transition phenomenon from the VSR to the ISR, similar to the one seen in Fig. 3 of ref. 11. Hitherto, it was not observed in ESS plots of longitudinal and transversal structure functions as both are dominated by the rank zero contribution d_n^0 which does show ESS.

For further support of this interpretation, we parametrize the $d_n^0(r)$ within Batchelor's parametrization,^(1, 12)

$$d_n^0(r) \propto D_n^M(r) \propto r^n \left[1 + \left(\frac{r}{r_c} \right)^2 \right]^{(-n+\zeta_n)/2} \quad (9)$$

$n=2, 4$. For the demonstrative calculation to follow we take $r_c = 10\eta$ and the She-Leveque model⁽¹³⁾ values $\zeta_2 = 0.70$, $\zeta_4 = 1.28$. Incompressibility gives $D_2^L(r) = r^{-3} \int_0^r D_2^M(\tilde{r}) \tilde{r}^2 d\tilde{r}$ and via Eq. (6) all other second order structure functions follow. For the fourth order moments, an analogous relation does not exist. However, within some closure approximations⁽⁹⁾ (whose nature is controversial), all 4th order structure functions follow from $D_4^L(r)$, cf. Eq. (2) of ref. 9. We stress that those relations are not generally true and their consequence that all 4th order structure functions scale the same is in direct contradiction to our findings and those of others. However, for the demonstration of transitional effects, for which the different intermittency in the ISR does not matter, Eqs. (2a)–(2c) of ref. 9 could be useful. Employing them we derive an ODE for $D_{1111} = D_4^L$,

$$D_4^M = 5D_4^L + \frac{11}{6} r \frac{d}{dr} D_4^L + \frac{1}{6} r^2 \frac{d^2}{dr^2} D_4^L \quad (10)$$

which can numerically be solved for the given $D_4^M(r)$ of Eq. (9). With ref. 9

$$D_{1122} = \frac{1}{3} D_4^L + \frac{r}{12} \frac{d}{dr} D_4^L \quad (11)$$

$$D_{2222} = D_4^L + \frac{9}{16} r \frac{d}{dr} D_4^L + \frac{1}{16} r^2 \frac{d^2}{dr^2} D_4^L \quad (12)$$

and Eqs. (7)–(8) all other fourth order moments follow. The resulting compensated ESS plots are shown in Fig. 3. Indeed, in the ESS plot c_2/a_2^2 vs a_2 a bump occurs at the VSR-ISR transition, similar to what we found in the numerical simulation. All other shown compensated ESS plots are dominated by $D_4^M = \sqrt{5} c_0$ and $D_2^M = 3a_0$, and therefore display ESS, as c_0

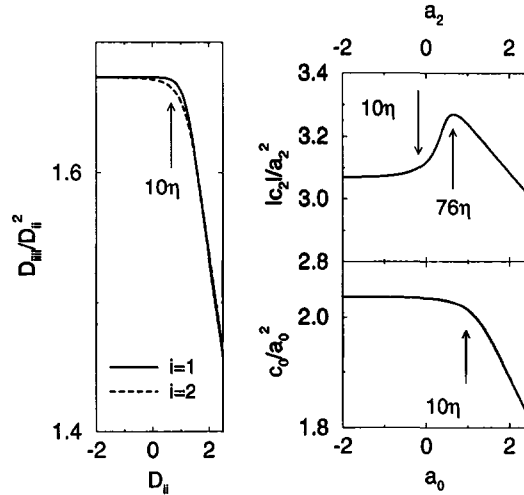


Fig. 3. Compensated ESS plots following from the Batchelor parametrizations (9) and Eqs. (2) of ref. 9. The curve c_2/a_2^2 vs a_2 is the only ESS plot which is not dominated by the tensors of rank zero and it does show a bump at the VSR-ISR transition. That the ISR scaling exponent ρ_i is the same for the four curves shown here for demonstrative reasons is a trivial consequence of the closure assumptions of ref. 9, but does not hold for the real data.

vs a_0 does. After the functional shape of the ESS transition from VSR to ISR in D_4^M vs D_2^M is now believed to be rather universal, it would be worthwhile to analyze in various experimental and numerical flows, whether the first angular contribution, i.e., c_2 vs a_2 , also is somehow universal and thus displays the type of structure that we found in Fig. 2b.

We now come back to the numerical results and focus on the ESS scaling exponents of Fig. 2 which we denote by $\rho_i = (\zeta_4^i - 2\zeta_2^i)/\zeta_2^i$, $i = L, T, M$ or $i = 0, 2$. The deviation of the ρ_i from zero characterizes the degree of intermittency of the corresponding moment. We find $\rho_L = -0.15$, $\rho_T = -0.30$ and $\rho_M = \rho_0 = -0.25$, $\rho_2 = -0.5$, again showing that the degree of intermittency is higher in the d_n^l with larger l . The She-Leveque model value (with the original She-Leveque parameters adopted to the longitudinal structure function)⁽¹³⁾ for ρ is $\rho = -0.16$.

We checked the possibility of scaling behavior if amplitudes corresponding to different irreducible subspaces are mixed: we do *not* find ESS if we plot structure functions $d_4^l/(d_2^l)^2$ vs d_2^l with *different* $l \neq l'$.

It will not have escaped the reader's attention that the simultaneous assumption of pure scaling behavior of both the $D_4^{L, T, M}$ as well as the $c_4^{0, 2, 4}$ is self contradictory if the exponents with different l are different. We follow L'vov *et al.*'s argument that the d_n^l are the more fundamental structure

functions and (employing Eq. (7) and incompressibility) write the ratios $D_4^{L,T}/(D_2^{L,T})^2$ as a sum of ratios of the d_n^L ,

$$\frac{D_4^L}{(D_2^L)^2} \propto \frac{c_0}{a_0^2} + 2 \sqrt{\frac{5}{7}} \frac{c_2}{a_0^2} + \sqrt{\frac{8}{7}} \frac{c_4}{a_0^2} \quad (13)$$

$$\frac{D_4^T}{(D_2^T)^2} \propto \frac{c_0}{a_0^2} - \sqrt{\frac{5}{7}} \frac{c_2}{a_0^2} + \frac{3}{4} \sqrt{\frac{2}{7}} \frac{c_4}{a_0^2} \quad (14)$$

From our numerics (see Fig. 1) the first term is found to be the leading order term. It represents the scaling of the modulus structure functions Eq. (4). In the first (and larger) correction term the approximation $a_0 \approx 11a_2$ (resulting from $\zeta_2 \approx 2/3$ and incompressibility) can be made, leaving only ratios whose scaling we can determine from the ESS-plots Fig. 2b; (the c_4 -term hardly contributes for large r). With that approximation the qualitative features of Fig. 2a can be understood from Eqs. (13) and (14): As $c_2(r) < 0$ the c_2/a_0^2 correction term to the leading c_0/a_0^2 term is negative [positive] for $D_4^L/(D_2^L)^2$ [$D_4^T/(D_2^T)^2$], leading to a less steep [steeper] “apparent” slope for the ESS exponents $\rho_L = -0.15$ [$\rho_T = -0.30$] of the longitudinal [transversal] structure function compared to the leading contribution with $\rho_0 = \rho_M = -0.25$. Even the fact that the correction to $\rho_0 = -0.25$ is twice as big for the longitudinal structure function as for the transversal one can be seen from Eqs. (13) and (14).

Finally, we would like to estimate the Reynolds number for which two distinct scaling regimes (in r) may be observable in $D_4^{L,T}$. Therefore, we plug in the scaling laws

$$\frac{c_i}{a_i^2}(r) = \frac{c_i}{a_i^2}(L) \left(\frac{r}{L}\right)^{\zeta_2 \rho_i}; \quad i = 0, 2 \quad (15)$$

and obtain with the numerical values at $r = L$, $c_0/a_0^2 \approx 6$ and $c_2/a_2^2 \approx -100$,

$$r^{\zeta_2 \rho_L} \frac{D_4^L}{(D_2^L)^2} \propto r^{\zeta_2 \rho_0} \left(1 - \alpha \left(\frac{r}{L}\right)^{\zeta_2(\rho_2 - \rho_0)} + c_4\text{-corr.} \right) \quad (16)$$

$$r^{\zeta_2 \rho_T} \frac{D_4^T}{(D_2^T)^2} \propto r^{\zeta_2 \rho_0} \left(1 + \frac{1}{2} \alpha \left(\frac{r}{L}\right)^{\zeta_2(\rho_2 - \rho_0)} + c_4\text{-corr.} \right) \quad (17)$$

We get $\alpha \sim 0.2$, $\zeta_2(\rho_2 - \rho_0) = \frac{2}{3}(-0.5 + 0.25) \approx -0.17$. Note that for small enough r the second term in (17) may dominate the first one and for even smaller r the third term will contribute. [In Eq. (16) the situation is more complicated as the second term has negative sign, but the lhs is positive definite.] Therefore, in principle $D_4^T/(D_2^T)^2$ shows several different scaling regimes. However, it will be very hard to detect these different

regimes as the required span of the Reynolds numbers is too large. In Eq. (17) the ratio L/r has to be as large as $L/r = (2/\alpha)^{1/0.17} \sim 10^6$ for the second term to overtake the first one. We put $r = \eta$ and estimate that this means $Re \sim 10^8$. This value would be hard to achieve in today's experimental or numerical flows, however, note that it strongly depends on the difference $\rho_2 - \rho_0$ which can only be measured with limited accuracy in low Reynolds number numerical simulations. What shall be detectable if L'vov *et al.*'s conjecture⁽⁸⁾ is right is that the apparent scaling exponents of the structure functions $D_n^{L,T}(r)$ or ESS scaling exponents thereof are slightly Re dependent whereas the scaling exponents of the irreducible objects $d_n^I(r)$ or their ESS exponents (the exponents of plots $|d_n^I(r)|$ vs $|d_m^I(r)|$) might well be universal, i.e., Reynolds number independent.

The main aim of this paper is to initiate measurements of such exponents as a function of Re up to very large Reynolds numbers⁽⁵⁾ to be able to decide whether the conventional structure functions $D_n^{L,T}$ or the irreducible structure functions $d_n^I(r)$ [which we favor because of their larger symmetry] are the more fundamental objects. We speculate that nature may have chosen an elegant way out of this decision, namely that in the large Reynolds number limit the scaling for *all* structure functions $D_n^{L,T,M}(r)$, $d_n^I(r)$ (for fixed n) may be the same.

ACKNOWLEDGMENTS

We thank I. Procaccia, K. R. Sreenivasan, and Leo Kadanoff for very helpful exchange. We in addition take great pleasure in expressing our gratitude to Leo Kadanoff for all he has taught us through his penetrating physical insight and originality, for his enduring support, and for his warm friendship. Our pleasure is doubled by having the opportunity to congratulate him on the occasion of his sixtieth birthday. Support for this work by the DFG under Grant SFB185-D3 and by the German-Israeli Foundation (GIF) is acknowledged, and also by the HLRZ Julich supplying us with the necessary computer time.

REFERENCES

1. A. S. Monin and A. M. Yaglom, *Statistical Fluid Mechanics* (The MIT Press, Cambridge, Massachusetts, 1975); L. D. Landau and E. M. Lifshitz, *Fluid Mechanics* (Pergamon Press, Oxford, 1987).
2. S. G. Saddoughi and S. V. Veeravalli, *J. Fluid Mech.* **268**:333 (1994).
3. J. Herweijer and W. van de Water, in *Advances in Turbulence V*, R. Benzi, ed. (Kluwer Academic Publishers, New York, 1995), p. 210; *Phys. Scripta* **T67**:136 (1996).

4. A. Noullez *et al.*, *J. Fluid Mech.* **339**:287 (1997); R. Camussi, D. Barbagallo, G. Guj, and F. Stella, *Phys. Fluids* **8**:1181 (1996); R. Camussi and R. Benzi, *Phys. Fluids* **9**:257 (1997).
5. B. Dhruva, Y. Tsuji, and K. R. Sreenivasan, *Phys. Rev. E* **56**:R4928 (1997).
6. O. N. Boratav and R. B. Pelz, *Phys. Fluids* **9**:1400 (1997); S. Chen, K. R. Sreenivasan, M. Nelkin, and N. Cao, *Phys. Rev. Lett.* **79**:2253 (1997).
7. S. Grossmann, D. Lohse, and A. Reeh, *Phys. Fluids* **9**:3817 (1997).
8. V. L'vov, E. Podivilow, and I. Procaccia, *Phys. Rev. Lett.* **79**:2050 (1997).
9. M. Ould-Rouis, R. A. Antonia, Y. Zhu, and F. Anselmet, *Phys. Rev. Lett.* **77**:2222 (1996).
10. R. Benzi *et al.*, *Phys. Rev. E* **48**:R29 (1993); R. Benzi, S. Ciliberto, C. Baudet, and G. R. Chavarría, *Physica D* **80**:385 (1995); R. Benzi *et al.*, *Physica D* **96**:162 (1996); G. Stolovitzky and K. R. Sreenivasan, *Phys. Rev. E* **48**:R33 (1993); M. Briscolini, P. Santangelo, S. Succi, and R. Benzi, *Phys. Rev. E* **50**:R1745 (1994); Ch. Meneveau, *Phys. Rev. E* **54**:3657 (1996).
11. S. Grossmann, D. Lohse, and A. Reeh, *Phys. Rev. E* **56**:5473 (1997).
12. G. K. Batchelor, *Proc. Camb. Philos. Soc.* **47**:359 (1951); H. Effinger and S. Grossmann, *Z. Phys. B* **66**:289 (1987); D. Lohse and A. Müller-Groeling, *Phys. Rev. Lett.* **54**:395 (1996).
13. Z. S. She and E. Leveque, *Phys. Rev. Lett.* **72**:336 (1994).